Variations of the Last Glacial Warm Pool: Sea surface temperature contrasts between the open western Pacific and South China Sea

Muhong Chen,[1] Qianyu Li,[2,3] Fan Zheng,[1] Xianzan Tan,[1] Rong Xiang,[1] and Zhimin Jian[2]

Received 27 May 2004; revised 22 January 2005; accepted 21 February 2005; published 3 May 2005.

[1] High-resolution paleoceanographic records from the southern South China Sea (SCS) and the tropical open western Pacific reveal multicentennial- to millennial-scale variations of the Western Pacific Warm Pool (WPWP) over the last 40 kyr. During the Last Glacial Maximum (LGM), in marine isotope stage (MIS) 2, planktonic *Globigerinoides sacculifer* $\delta^{18}O$ in core NS93-5 from the southern SCS and in core WP92-5 from the central WPWP registered a similar average value of about $-1.5‰$. However, the average $\delta^{18}O$ value was about 0.5‰ more negative in the SCS than in the central WPWP, as was their difference before and after the LGM in the later part of MIS 3 and early portion of MIS 1. These results indicate weaker monsoonal and fluvial effects on the southern SCS during the last glacial than during pleniglacial and postglacial periods owing to different oceanic circulation modes and regional topography. The calculated seasonal temperature differences of summer and winter sea surface temperatures (SSTs) between the open WPWP and the southern SCS were up to 3–4.5°C during the LGM but only slightly over 3°C in the southern SCS and less than 2°C in the open WPWP during other periods. From about 29 to 25 ka the MIS 2/3 transition was marked by a sudden SST increase in the southern SCS but a decrease in the open WPWP. Over this 4 kyr period the average annual SST appeared to be only 28°C in the central WPWP but more than 28°C in the southern SCS, indicating a shift of the central WPWP toward the far west during that time. Furthermore, our results imply a period of nearly 6 kyr from 22.5 to 16.5 ka without an apparent warm pool of 28°C in the western Pacific.

Citation: Chen, M., Q. Li, F. Zheng, X. Tan, R. Xiang, and Z. Jian (2005), Variations of the Last Glacial Warm Pool: Sea surface temperature contrasts between the open western Pacific and South China Sea, *Paleoceanography*, *20*, PA2005, doi:10.1029/2004PA001057.

1. Introduction

[2] As one of the most important forcing engines of the Earth climatic system, the western Pacific warm pool (WPWP) has received special attention from marine geoscientists in the last ten years, especially in using sedimentary records to study the WPWP's evolutionary history and environmental characters for the purpose of establishing a more convincing theory on the driving mechanisms of the climate system. Some previous works has indicated that the WPWP during the Last Glacial Maximum (LGM) had sea surface temperatures (SST) similar to today's [*CLIMAP Project Members*, 1981; *Anderson et al.*, 1989; *Thunell et al.*, 1994; *Thunell and Miao*, 1996], implying a constant WPWP remained throughout the last glacial cycle with very little effect from changes in the global climate system. Other studies, however, have shown up to ~5°C SST difference over the last 450 kyr [*Lea et al.*, 2000], with increases of 3.5–4.0°C during the last two glacial-interglacial transitions [*Visser et al.*, 2003], and sea surface salinities (SSS) that were ~1‰ higher in the LGM western Pacific due to excess evaporation [*Martinez et al.*, 1997]. The pattern of an abrupt termination of the last glacial period that occurred in high latitudes can also be found in low latitudes including the South China Sea (SCS) [*Broecker et al.*, 1988b; *Kienast et al.*, 2001]. A recent study of foraminiferal magnesium/calcium ratios in Deep Sea Drilling Hole 806B within the WPWP revealed a SST decrease by about 3°C in the LGM, with this low-latitude SST decrease preceding changes in continental ice volume by about 3000 years may suggesting a major role of tropical cooling in driving ice-age climate [*Lea et al.*, 2000]. Similar results were also recorded in core MD9821-62 from the Makassar Strait, Indonesia [*Visser et al.*, 2003] and is supported by glacial Mass balance modeling [*Steven and Clark*, 2000]. Any changes in the WPWP temperature and salinity would have been preserved in the biological and sedimentary records not only from the open ocean but also from marginal seas surrounding and within the WPWP.

[3] Located between the western Pacific and northern Indian Ocean parts of the warm pool, the southern South China Sea has several straits along its periphery that connect to the Sulu Sea, Java Sea and Indian Ocean. With typical tropical marginal marine environmental features, the SCS lies in a region presently characterized by one of the most brisk sea-air exchanges in the world ocean, affected by both the El Nino–Southern Oscillation climate phenomena as well as the East Asian summer monsoon. At the junction of three tectonic plate convergences, the SCS's formation and evolution are closely related to the uplift of the Tibetan

[1]South China Sea Institute of Oceanology, Chinese Academy of Sciences, Guangzhou, China.
[2]Laboratory of Marine Geology, Tongji University, Shanghai, China.
[3]Also at Department of Geology and Geophysics, University of Adelaide, Adelaide, South Australia.

0883-8305/05/2004PA001057

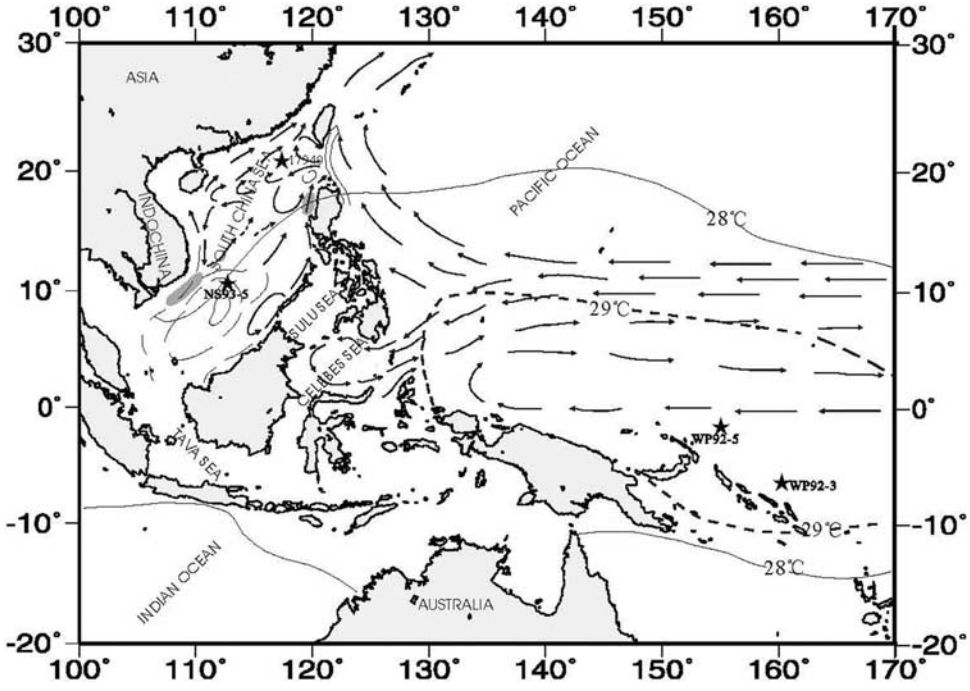

Figure 1. A map of the western Pacific showing modern surface circulation and SST isotherms of 29° (thick dashed line) and 28° (thin line) that denote the modern range of the WPWP [*Yan et al.*, 1992]. Also shown are the locations of cores NS93-5 and 17940 in the southern and northern South China Sea and cores WP92-5 and WP92-3 in the open central WPWP. The summer upwelling area in the SCS is shaded.

Plateau. Previous studies on SCS paleoceanography include stratigraphy documented by AMS ^{14}C dates [*Andree et al.*, 1986; *Broecker et al.*, 1988a] and local response to glacial-interglacial changes during the last deglaciation [*Broecker et al.*, 1988b; *Duplessy et al.*, 1991], SST [*Wang and Wang*, 1990], productivity [*Winn et al.*, 1992; *Thunell et al.*, 1992; *Jian et al.*, 1999], surface circulation and carbonate cycles [*Wang et al.*, 1995; *Wang*, 1999], monsoon changes and upwelling [*Wang et al.*, 1999; *Jian et al.*, 2001], climatic events linked to high-latitude records [*Wang et al.*, 1999; *Chen et al.*, 2000], and also its long-term geological history through Ocean Drilling Program (ODP) Leg 184 postcruise research [*Yang et al.*, 2002; *Wang et al.*, 2003; *Chen et al.*, 2003]. However, knowledge is still lacking especially regarding the contrast in paleoceanographic conditions between the SCS and the open western tropical Pacific in periods immediately leading to and after the LGM.

[4] The purpose of this study has been to compare paleoceanographic conditions over the last 40 kyr in the southern SCS and central WPWP by analyzing planktonic foraminiferal oxygen isotopes in high-resolution sampled cores, and to examine SST variations between these two areas and their implications in regional and global climate changes. To do so first requires development of a comparative age model for revealing and correlating paleoceanographic events in the region.

2. Material and Methods

[5] Core NS-93-5 was taken from 112°45.19′E and 9°59.94′N at a water depth of 1792 m, where the Nansha terrace lies on a gentle slope of only about 0.17° in the southern SCS. From an area outside the western Nansha reef region and remote from any big river mouth, relatively stable depositional conditions have led to the preservation of a hemipelagic sequence without obvious disruption or distortion that represents a normal marine depositional record from the southern slope terrace of the SCS (Figure 1). Continuous sampling at every 1 cm from the upper 150 cm and every 2 cm from 151–534 cm of core NS-93-5 was done in this study.

[6] Piston cores WP92-5 and WP92-3 are located at 155°01.16′E/2°02.59′S and 160°16.35′E/6°45.05′S, in water depths of 2345 m and 2180 m in the tropical western Pacific (Figure 1). The pelagic to hemipelagic sediments are mainly composed of silty nannofossil ooze and clay silt in alternating yellowish brown and blackish brown layers, interbedded with some greenish gray with yellowish brown bands. Samples at 1 cm spacing were taken continuously from the 165 cm long WP92-5 and from the 61-cm-long WP92-3.

[7] For oxygen isotope analyses, we used all samples collected from the three cores. About 10 individuals of the planktonic foraminifer *Globigerinoides sacculifer* in the 250–350 μm fraction were picked. After processing with conventional methods, the foraminifer tests were analyzed using a Finnigan MAT251 mass spectrometer in the Open Laboratory of Marine Sediments, Qingdao Institute of Marine Geology, Ministry of Land Resources. Foraminifer population analyses were done on alternating samples. Paleotemperatures were estimated using transfer function FP-12E [*Thompson*, 1981], the modern analog technique or

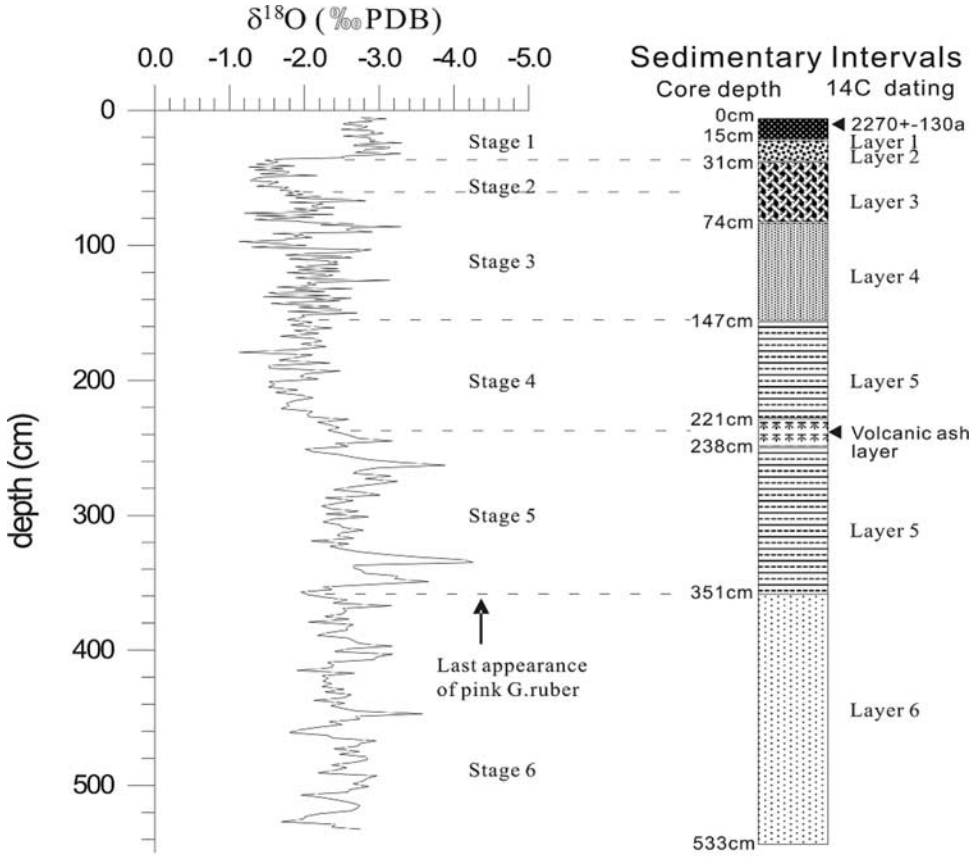

Figure 2. Correlation between sediment layers based on colors and oxygen isotopic stratigraphy in core NS93-5. The volcanic ash layer represents the Toba eruption that occurred at the transition of oxygen isotopic stages 4 and 5.

MAT [*Prell*, 1985], and the SIMMAX-28 method [*Pflaumann and Jian*, 1999]. The foraminiferal fauna composition from these three cores were not obviously affected by the calcium carbonate dissolution, because all core sites are shallower than the 3000 m lysocline depth and 4000 m compensation depth in the SCS [*Chen and Chen*, 1989] as well as the greater depths of these dissolution levels in the tropical Pacific [*Heath*, 1970].

[8] Eighty-eight samples from core WP92-5 at 2.5 cm spacing were taken for geomagnetic study, after removing the topmost and the lowermost 2.5 cm that might have been disturbed. Among these, 64 samples were collected sequentially and vertically from the top to the bottom of the core with standard paleomagnetic sampling cylinders. In addition, 15 parallel box ($2 \times 2 \times 2$ cm) samples were taken respectively from the upper 10–20 cm, middle 75–85 cm and lower 45–155 cm intervals, and 9 random samples from other layers of the core were collected for improving the resolution. The natural residual magnetization (NRM), magnetic inclination and magnetic declination were measured using a 2G-755R mode low-temperature superconductive magnetometer in the Paleogeomagnetism Laboratory of the Geological and Geophysical Institute, Chinese Academy of Sciences (CAS).

[9] Three bulk sediment samples from core NS93-5 and three samples from WP92-5 were measured for conventional ^{14}C ages by Guangzhou Institute of Geochemistry, CAS.

3. Results and Discussion

3.1. Major Sedimentary, Biostratigraphic, and Isotopic Characteristics of Core NS-93-5

[10] The 534-cm-long NS93-5 is composed of silt and clay-rich sediments with abundant microfossils including foraminifera, radiolarians and diatoms. A total of 6 major intervals can be divided mainly on the basis of sediment colors that probably correspond to deposition under different environmental conditions (Figure 2). A thin volcanic glass layer that occurs at 221–238 cm within the 5th interval represents the famous Toba eruption widely recorded in the Indo-west Pacific region [*Ninkovitch and Donn*, 1976; *Rampino and Self*, 1993; *Zielinski et al.*, 1996]. The Toba eruption occurred about 71 kyr ago [*Zielinski et al.*, 1996], straddling the interstitial 19/20 boundary(=MIS 4/5 boundary).

[11] Strong swings in the oxygen isotopic record of *G. sacculifer* from core NS-93-5 indicate a large range of climate changes in marine isotopic stages (MIS) 1 to 6 (Figure 2). The basic definition of oxygen isotopic stages for the last two glacial cycles proposed by *Prell et al.* [1986] and *Martinson et al.* [1987] are followed in this study. Ages

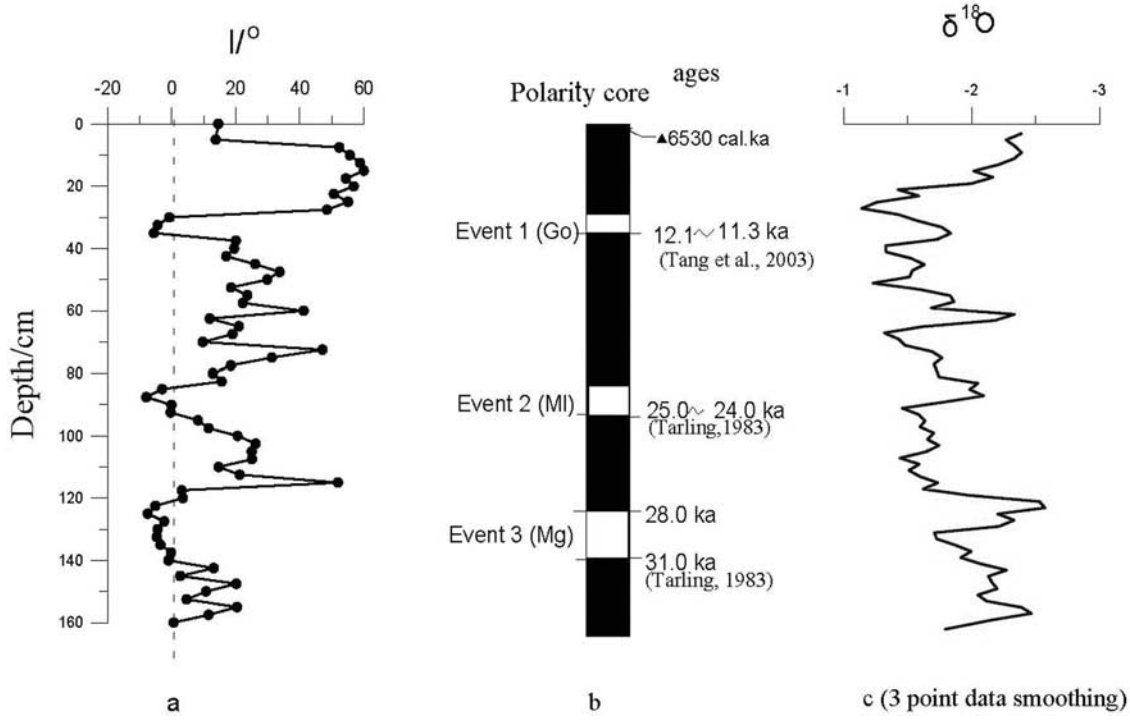

Figure 3. Magnetostratigraphy and oxygen isotopic curve from coreWP92-5: (a) magnetic inclination; (b) the polarity column with three negative magnetic reversal events; and (c) the smoothed $\delta^{18}O$ curve. Go, Gothenburg; Ml, Mono Lake; Mg, Lake Mungo or Maelifell.

for MIS 1–3 were estimated by reference to the age model of core 17940 [*Wang et al.*, 1999], which was established by tuning the negative $\delta^{18}O$ peaks to warm Dansgaard-Oeschger (D-O) events 1–10 in ice core. The GISP-2. MIS 1, with $\delta^{18}O$ varying between −2.5 and −3.0‰ occupies the uppermost 35 cm of the core. $\delta^{18}O$ values from MIS 2 increase to about −1.5‰ while MIS 3 spans the interval of 59–147 cm with $\delta^{18}O$ mostly varying between −1.70 and −2.50‰. Increasing $\delta^{18}O$ values generally between −1.5 and −2.0‰ are recorded for MIS 4 down to its base at 233 cm with a more negative value of −2.46‰, at about 73.9 ka [*Martinson et al.*, 1987]. The Toba volcanic ash layer lies exactly at the MIS 4/5 transition, with an age of 71 ka [*Huang et al.*, 1999; *Lee et al.*, 1999], though it was earlier dated as 73.5 ka [*Michael and Stephen*, 1992]. MIS 5 is characterized by three large $\delta^{18}O$ swings between 233 and 355 cm, and all subsidiary events of *Martinson et al.* [1987] can also be distinguished. The bottom part of the core, between 355 and 534 cm, is interpreted as belonging in MIS 6 or older with $\delta^{18}O$ values mostly between −1.7 and −3.0‰. The appearance of pink *G. ruber* in this interval supports this conclusion as its extinction ~120 ka from the Indo-Pacific region has been dated by *Thompson et al.* [1979] and many subsequent studies. Compared to other southern SCS records (e.g., 17957-2 [*Jian et al.*, 2000]; MD972142 [*Wei et al.*, 2003], the relatively negative $\delta^{18}O$ values from the bottom part of NS93-5 is unusual. Further studies are pending to clarify whether these more negative $\delta^{18}O$ values represent instead may interglacial MIS 7 or that perhaps glacial MIS 6 was influenced more by lower salinity conditions due to enhanced freshwater discharge when the SCS was closed in the south during previous glacial lowstands [*Chen et al.*, 2000].

3.2. Magnetostratigraphy and ^{14}C Dates for Core WP92-5

[12] Magnetic inclinations under the demagnetized field from 35 mT to 40 mT were selected as the basis for magnetostratigraphic division of core WP92-5 because the residual magnetization intensity (Mr) obtained under this demagnetized field makes up about 40–50% of the NRM, and the measured magnetic inclination is relatively stable. The results shown in Figure 3 indicate three major magnetic polarity reversal events correlated to the calibrated ^{14}C age and oxygen isotope stratigraphy.

[13] Reversal event 1 occurs at 35–30 cm with three negative magnetic inclinations, −0.8°, −4.5° and −5.6°, interpreted here as representing the Gothenburg geomagnetic excursion with an age of about 12.1–11.3 [*Tang et al.*, 2003]. Many observed geomagnetic reversals appear to be different in age between sites from different latitudes [*Clement*, 2004], and this is true for the age for the Gothenburg. By reference to *Tarling*'s [1983] estimated age of 13.0–11.0 ka, the event recorded in cores NS89-76 and NS87-11 from the low-latitude SCS between 7° and 5°N has been considered to be at 12.0–11.0 ka [*Tang et al.*, 1997], but its equivalent age in cores QC1, QC2 and QC3

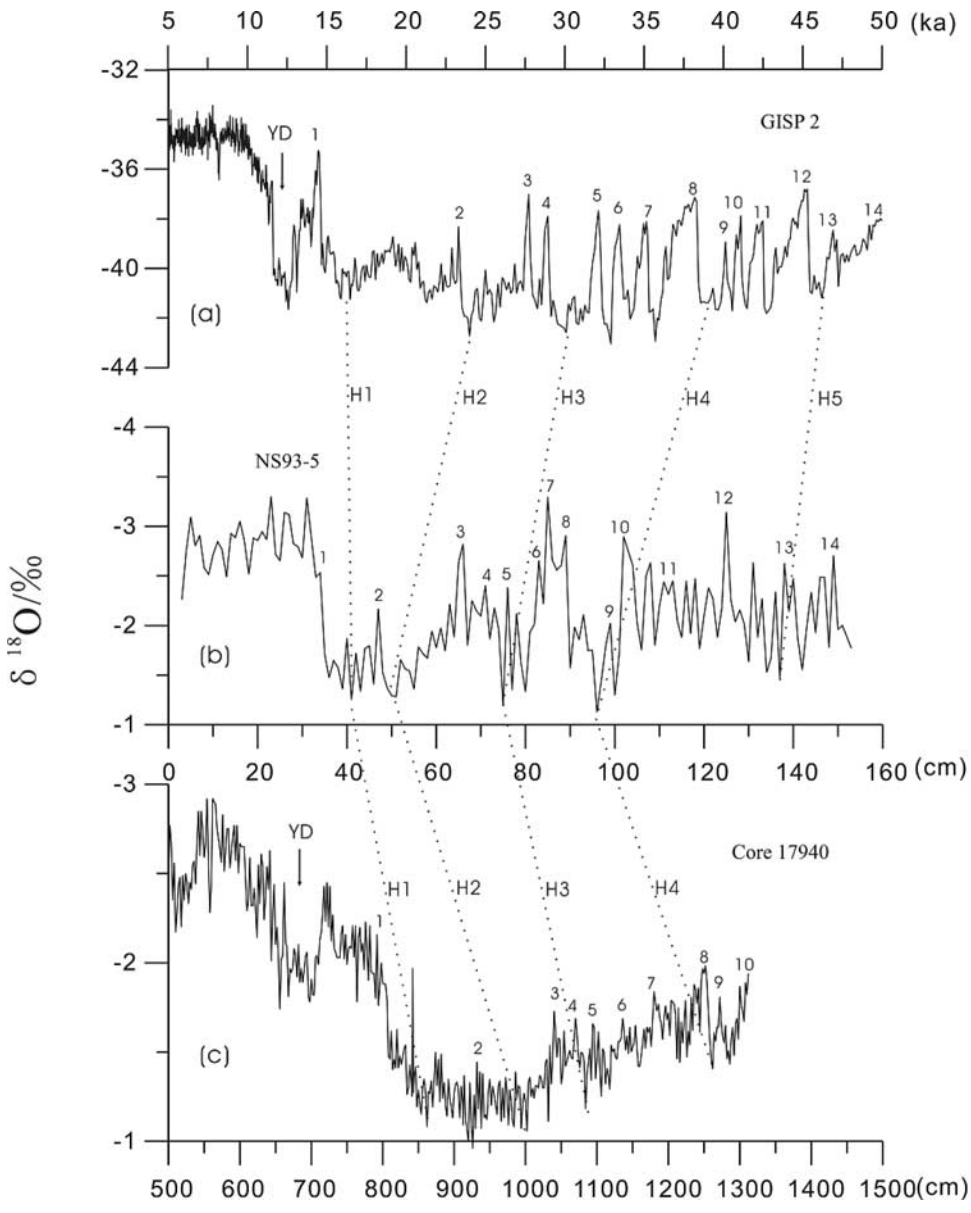

Figure 4. Correlation of D-O and Heinrich events between the Greenland ice core GISP2, northern SCS core 17940, and southern SCS core NS93-5 using oxygen isotope stratigraphy. The age models for GISP2 and core 17940; the latter constrained by AMS ^{14}C dates. Comparison of the small-scale climatic warming (D-O) and cooling (H) events between these two cores and NS93-5 improved the accuracy of the age model for NS93-5.

from the Yellow Sea between 32° and 37°N may be slightly older, at 12.5–11.0 ka [*Zhou and Ge*, 1987].

[14] Reversal event 2 from 95–85 cm is marked by four negative inclinations: −3.02°, −7.97°, −0.11°, and −0.37°, interpreted as equivalent to the Mono Lake geomagnetic excursion (Figure 3a). The age for this event has been dated at 25.3–24.0 ka in the Arctic Ocean by *Nowaczyk et al.* [2001], 28–27 ka in Greenland Sea II core by *Nowaczyk* [1997], and 25.0–24.0 ka from earlier syntheses by *Tarling* [1983] and *Jacobs* [1994]. Considering the calibrated ^{14}C age of 30.6 calendar (cal) ka at 112.5 cm in WP92-5, the age for this event from 95 to 85 cm of the same core can be estimated to have occurred at about 28–27 ka. Comparably, its position lying about 15 cm below the H2 event in isotopic stratigraphy, dated at 26 ka, may imply that the Mono Lake event in the SCS region was as much as ~2 kyr older, at 28 ka, if an average sedimentation rate of 7 cm/kyr (see below) is followed for core WP92-5 (Figure 3).

[15] Reversal event 3 from 140 to 122.5 cm (Figure 3a), as indicated by eight negative magnetic inclinations (−5.16°, −7.51°, −2.42°, −4.45°, −4.73°, −3.51°, −0.23°) and −1.09°, is considered to represent the Lake Mungo or Maelifell geomagnetic excursion with an age of 31–28 ka according to *Tarling* [1983]. However, the

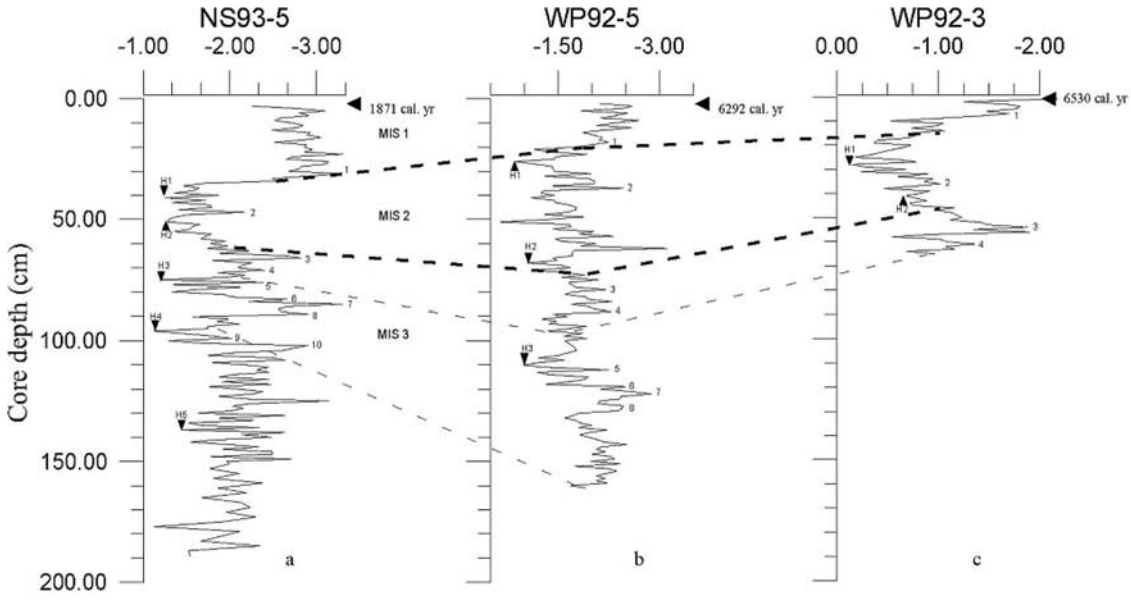

Figure 5. Comparison of D-O (1 to 10) and Heinrich (H1 to H5) events in southern SCS core NS93-5 and western Pacific cores WP92-5 and WP92-3. The thick dashed lines show the boundaries of marine oxygen isotopic stages. The fine dashed line links the base of WP92-3 to its approximate position in other cores.

presence of the H3 isotopic event at 110 cm, which occurred about 30 ka [*Grootes and Stuiver*, 1997; *Wang et al.*, 1999], suggest that the Lake Mungo geomagnetic excursion from 140 to 122.5 cm in core WP92-5 may bear an age of 35–32 ka in this area. If the latter estimate is valid, the bottom of the core at 160 cm should have an age of about 37 ka based on an estimated average sedimentation rate of ~7 cm/kyr.

3.3. Summary of the Age Model for NS93-5 and WP92-5/WP92-3

[16] In addition to the magnetostratigraphic, biostratigraphic and event-stratigraphic constraints discussed above, the age model of core 17940, constrained by AMS ^{14}C ages [*Wang et al.*, 1999], is used for correlation with NS-93-5 and WP92-5/WP92-3. Core 17940 (117°23.0′E, 20°07.0′N, water depth 1727 m) is located on the northern slope of the SCS. From this core, *Wang et al.* [1999] obtained 40 calendar ages by converting their AMS ^{14}C results over the 1272.5 cm section that spans the last 40 kyr (Figure 4). By tuning the negative δ^{18}O peaks that signal the warm Dansgaard-Oeschger (D-O) events 1 to 10 and the positive δ^{18}O peaks that signal the cold Heinrich events, correlations between cores 17940 [*Wang et al.*, 1999] and NS93-5 and the GISP2 ice core record were used to establish a better chronostratigraphy for NS93-5 (Figure 4), as well as for cores WP92-5 and WP92-3 from similar calibrations (Figure 5) [*Chen et al.*, 2000]. This practice has enabled a re-assessment of the ages for the three magnetic reversal events to be 20.77–19.22 cal ka for event 1, 29.93–29.27 cal ka for event 2, and 38.06–35.39 cal ka for event 3, probably corresponding to the Gothenburg event, the Mono Lake event and the Mungo event respectively in the western tropical Pacific.

[17] Sedimentation rates for core WP92-5 could then be derived from linear interpolation between the age control points deduced from tuning to D-O events, and the results show sedimentation rates for MIS 1, MIS 2 and MIS 3 of 1.75 cm/kyr, 4.92 cm/kyr and 7.99 cm/kyr, respectively. The average sedimentation rate for the last 38 kyr at WP92-5 is about 5 cm/kyr. At core NS93-5, the corresponding sedimentation rates are 2.27 cm/kyr, 2.15 cm/kyr, 3.28 cm/kyr and (average) 2.61 cm/kyr for MIS 1, 2 and 3, respectively. Therefore, based on the sedimentation rates and the interval lengths of cored samples in each oxygen isotope stage, the sampling analysis resolutions for MIS 1, 2 and 3 were calculated as 571, 203 and 125 years for core WP92-5, and 441, 465 and 304 years for core NS93-5, respectively.

3.4. Surface Water Variations Indicated by δ^{18}O

[18] The planktonic δ^{18}O record appears to have been strongly affected by salinity changes in the SCS and less so by global ice volume as calculated using a benthic δ^{18}O stratigraphy [*Wang et al.*, 1999]. On the basis of *G. sacculifer* δ^{18}O, *Martinez et al.* [1997] estimated that salinity in the WPWP during the Last Glacial Maximum was about 1‰ higher than today's, implying higher evaporation relative to precipitation over much of the LGM in the region. Accordingly, the *G. sacculifer* δ^{18}O records from cores NS93-5, WP92-5 and WP92-3 (Figure 6) indicate local responses to global climatic changes since the last glacial at different oceanographic and fluvial settings where salinity changes appear to have been influential.

[19] The δ^{18}O records for MIS 2 from NS92-5 and WP92-5 are similar in having an average value of about −1.5‰, which is 0.2‰ more negative than the record from the

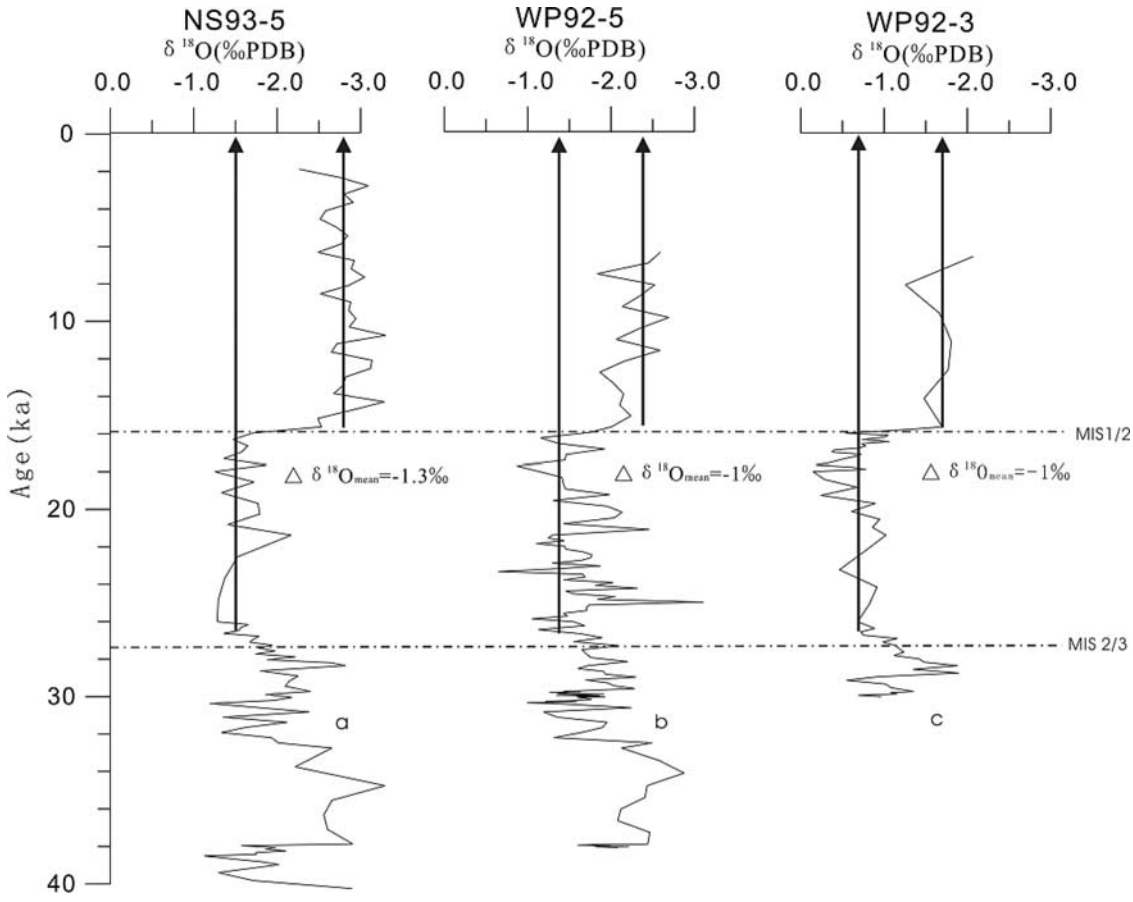

Figure 6. Comparison of $\delta^{18}O$ values between (a) core NS93-5 from the southern SCS and cores (b) WP92-5 and (c) WP92-3 from the open central WPWP. The average $\delta^{18}O$ values for MIS 1 and MIS 2 are shown by arrows, and their differences as "$\geq\delta^{18}O_{mean}$," respectively.

northern SCS core 17940 over the same period [*Wang et al.*, 1999]. These observations probably indicate similar surface water conditions with little fluvial influence in the central part of the SCS during the LGM, and similar water temperatures across the southern SCS and open WPWP, although the temperature in the northern SCS could be as much as 1°C lower. Higher $\delta^{18}O$ values are systematically recorded in core WP92-3: -1.258 to -2.072‰ for MIS 1, -0.2‰ to -1‰ for MIS 2, and -0.549 to -1.898‰ for MIS 3, likely due to stronger evaporation and a higher salinity at this site throughout the glacial-interglacial cycles [*Martinez et al.*, 1997]. A higher salinity at the core WP92-3 locality is consistent with previous findings that sea-surface salinity generally increased with latitude from north to south in the WPWP during both the LGM and the Holocene [*Martinez et al.*, 1997, Figure 10]. However, why the relatively short distance between WP92-5 and WP92-3 is marked by such a noticeable offset in $\delta^{18}O$ values ($\sim$0.6‰) in the Holocene-LGM period is unclear at present. Modern temperatures are similar and evaporation can hardly be invoked to explain such a large difference. Some unusual current or other unknown cause may have occurred during these periods and will hopefully be identified with further work.

[20] Large $\delta^{18}O$ differences exist between MIS 1 samples from NS93-5 and WP92-5 (Figure 6). During MIS 1 the average and minimum $\delta^{18}O$ values are about -2.8‰ and -3.3‰ from core NS93-5, and -2.3‰ and -2.75‰ from core WP92-5, respectively. Different $\delta^{18}O$ values, with a similar magnitude offset, also occurred in MIS 3 between these two sites. On average, the $\delta^{18}O$ at the locality of NS93-5 is about 0.5‰ more negative than at WP92-5. More negative $\delta^{18}O$ values at NS93-5 cannot be attributed to the effect of temperature because SST in many parts of the SCS are lower than in the open western Pacific where the center of the WPWP is located. It is suggested instead that during warm periods, summer monsoon-derived fluvial inputs from rivers such as the Mekong River brought increased amounts of freshwater into the southern SCS, causing lower salinities and more depleted $\delta^{18}O$ values in foraminifera. This situation did not occur in the open western Pacific, and was even less likely to occur in the glacial SCS because of weak rainfall in the winter monsoon period.

[21] These results match well with observations from global atmospheric circulation models [*Miller and Russell*, 1990] and oceanic circulation models for the LGM in the WPWP area [*Lautenschlager et al.*, 1992; *Martinez et al.*, 1997], and especially with those published previously from

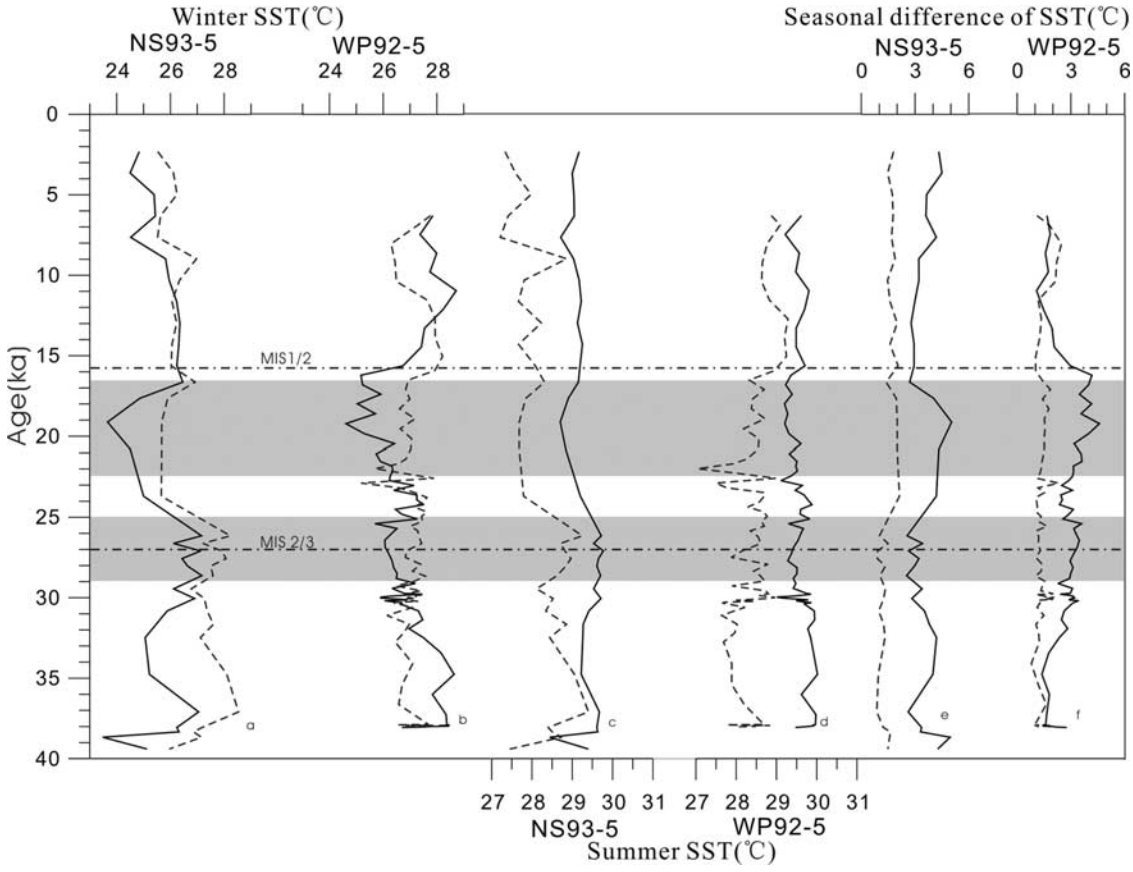

Figure 7. Results of SST estimates using the FP-12E method (solid lines) and MAT method (dashed lines) for NS93-5 from the southern SCS and WP92-5 from the open central WPWP: (a and b) winter SST, (c and d) summer SST, and (e and f) seasonal SST differences. The average values are indicated by arrows.

the SCS [*Wang and Wang*, 1990; *Wang et al.*, 1995]. The SCS presently receives highly saline North Pacific surface water that accumulates in the southern part of the basin during Northern Hemisphere winter, but the surface circulation is reversed during northern summer so that the highly saline surface water is replaced by fresher water coming from the south [*Miyama et al.*, 1996]. In a glacial scenario, the southern seaways connecting the SCS and the Indian Ocean were closed [*Wang et al.*, 1995; *Chen et al.*, 2000], and the highly saline North Pacific water could not have been replaced because fresher water was limited. Thus, while the $\delta^{18}O$ variations in core WP92-5 mainly reflect ice volume and seawater temperature changes, those in core NS93-5 are largely influenced by salinity variations triggered by monsoon changes.

[22] *Wei et al.* [2003] attributed the $\delta^{18}O$ difference between core MD972142 in the southern SCS and ODP Site 769 in the Sulu Sea to the influence of summer monsoons that increased precipitation and freshwater discharge to the SCS. The $\delta^{18}O$ differences, or $\Delta\delta^{18}O_{MD142}$ - $\delta^{18}O_{ODP769}$, decrease to 0–0.5‰ during glacials but increase to 0.5–1.5‰ during interglacials. The inference of a stronger winter monsoon during glacial and a stronger summer monsoon during interglacial periods is consistent with earlier results from the SCS [*Wang and Wang*, 1990; *Huang et al.*, 1997; *Wang et al.*, 1999; *Jian et al.*, 2001]. These $\delta^{18}O$ records provide a marine proxy of the East Asian monsoon variations comparable to the magnetic susceptibility record from the Chinese Loess Plateau [*Wei et al.*, 2003].

[23] The $\delta^{18}O$ fluctuations presented here from the southern SCS and central WPWP (Figure 6) provide further insight into the summer monsoon activity and its relationship with warm pool variations. As discussed further below, our results show more variable climate conditions and monsoon activities during MIS 2 and 3 and a relatively stable MIS 1 within and around the western margin of the WPWP.

3.5. SST Variations

[24] Transfer function FP-12E by *Thompson* [1981] used in many studies for calculating paleotemperature in the SCS area has been shown to yield consistent good results with oxygen isotopic features [*Miao et al.*, 1994; *Jian et al.*, 1998b; *Steinke et al.*, 2001]. Recently, a new transfer technique SIMMAX-28 was specifically developed for the

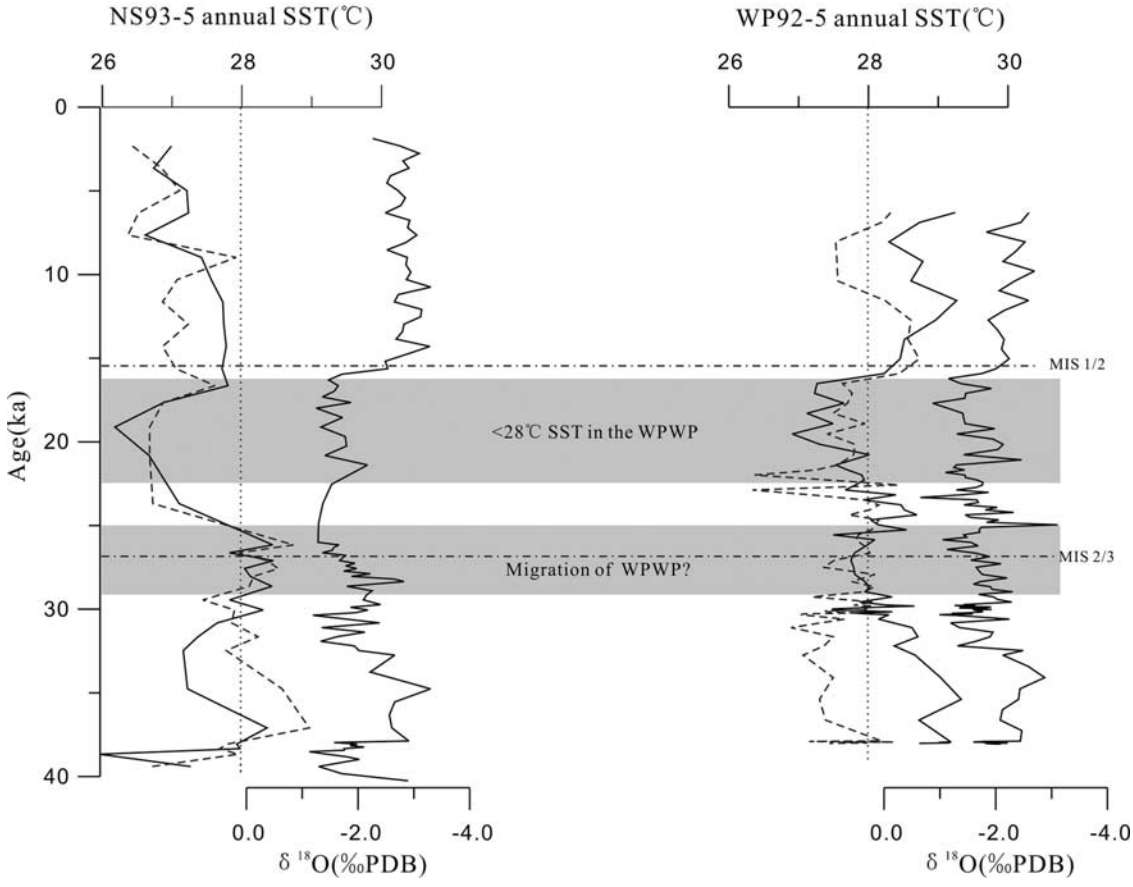

Figure 8. The $\delta^{18}O$ curves and mean annual SST arranged against age for NS93-5 from the southern SCS and WP92-5 from the open central WPWP. Solid lines show $\delta^{18}O$ curves and mean SST by the FP-12E method; dashed lines are SST values by the MAT method.

western Pacific area, which has resulted in smaller estimates of temperature change [*Pflaumann and Jian*, 1999; *Wang*, 1999]. *Steinke et al.* [2001] compared three different foraminiferal transfer functions (SIMMAX-28, RAM, FP-12E) with geochemical ($U^{k'}_{37}$) SST estimates for the tropical SCS and found that the best relationship exists between the $U^{k'}_{37}$ and the FP-12E estimates. Although equation FP-12E has a relatively larger standard error, its calibration data set included low-latitude samples in the western North Pacific that makes it suitable for use with SST reconstructions in the SCS and tropical Pacific region. It gave better sensitivity of SST reconstruction for these areas in our analysis. The lower sensitivities of SIMMAX-28 and RAM methods and their tendency to that underestimate the glacial cooling could be due to the lack of suitable analogs from temperate to subpolar regions in the data set used for calibration of these two transfer functions [*Steinke et al.*, 2001]. For these reasons, we mainly use the results calculated with transfer function FP-12E, which produced the winter and summer temperatures for NS93-5 and WP92-5 shown in Figure 7.

[25] For core NS93-5 from the southern SCS, the estimated winter and summer paleotemperatures show a similar variation trend although with different amplitudes. Winter temperatures fluctuated in the range of 24.5–26.5°C for MIS 1, about 23.5–26.5°C for MIS 2, and 25–27°C for MIS 3, or a drop of about 1–3°C in the LGM. Although reaching a low of 28.7°C in the LGM, summer temperatures remained relatively stable, averaging 29.2°C for all the three periods. Thus the seasonal temperature difference between winter and summer varied from 2.5°C to 4.5°C in MIS 3, increased to near 5°C in MIS 2 (LGM), and was reduced to 2.5–4.5°C in MIS 1.

[26] In core WP92-5 from the central WPWP, summer temperatures fluctuated in a narrow range of 29–30°C over the last 38 kyr. Winter temperature variations show distinct glacial-interglacial patterns, from about 28°C in MIS 3 to near 24.5°C in the LGM and to more than 28°C in the early Holocene. The seasonal temperature difference between winter and summer was over 3°C in the LGM, and less than 2°C in MIS 1 and 3 mainly due to lower temperatures in winter (Figure 7).

[27] By calculating the average SST variations in the SCS, Sulu Sea and other localities of the western Pacific between 5° and 20°N, *Wang* [1999] concluded that winter SST at the LGM was much cooler in the western Pacific marginal seas than in the open ocean at the same latitudes, whereas the summer SST was similar between the two regions, resulting in a much larger seasonality during the LGM in the marginal seas. Our results from

NS93-5 and WP92-5, however, indicate that winter temperature differences between the open Pacific and southern SCS remained high not only in glacial but also in interglacial periods. For example, early Holocene winter temperatures varied between 27.5°C and 29°C in central WPWP core WP92-5 and between 25.5°C and 26.5°C in southern SCS core NS93-5, with at least 2°C winter temperature difference between these two areas (Figure 7). The decreasing SCS winter temperature during the early to mid-Holocene was likely due to the effect of an enhanced East Asian winter monsoon [*Wang et al.*, 1999; *Jian et al.*, 2001], which may have been echoed also in the central WPWP as well as other marginal seas in the region.

[28] It is noteworthy that winter and summer SST around the MIS 2/3 transition increased in the southern SCS while in the central WPWP the winter SST remained low or even decreased slightly, an event persisting nearly 4 kyr from 29 ka to 25 ka (Figure 7). This abnormal phenomenon resulted in a higher winter SST in the southern SCS than in the open Pacific, indicating that an unusual climate condition prevailed in the WPWP at that time.

[29] The modern WPWP has a mean annual sea surface temperature of >28°C [*Yan et al.*, 1992]. If we take 28°C as the minimum SST threshold for what constitutes the ''warm pool,'' the persistent presence of the warm pool during the LGM and earliest Holocene appears to be doubtful. The mean annual SST curves shown in Figure 8 indicate that, from the LGM to MIS 2/1 transition, SST dropped to about 27°C in the central WPWP but rose to almost 28°C in the southern SCS. This contrast may imply a more contracted WPWP in the LGM and the earliest Holocene than previously thought. The center of the warm pool migrating westward next to the southern SCS in the last glacial and immediate postglacial periods may not be implausible especially when the monsoon system started to shift from a winter monsoon dominance to a summer monsoon dominance. The period with 27°C annual SST in the central WPWP persisted for about 6 kyr, from about 22.5 ka to 16.5 ka. Similar results have been reported from the Okinawa Trough where the warm Kuroshio Current has been influential since about 16 ka during the last glaciation [*Li et al.*, 2001, Figure 6]. Before 16 ka, however, the Kuroshio was not present in the Okinawa Trough at sea level lowstands due to the existence of a land bridge connecting the central-southern Ryukyu Arc and Taiwan [*Ujiié et al.*, 1991; *Jian et al.*, 1998a; *Ujiié and Ujiié*, 1999]. Furthermore, the SST decrease of about 3°C [see also *Lea et al.*, 2000] in the tropical western Pacific during the LGM indicates a different mode of the WPWP at that time compared to today.

4. Summary

[30] Paleoceanographic changes in the southern SCS and the open western Pacific have been studied on the basis of oxygen isotope analysis of planktonic foraminifera in cores NS93-5, WP92-5 and WP92-3. Continuous sampling at about 1 cm spacing provides multicentennial to millennial-scale resolution of about 304 to 465 years for core NS93-5, and 125 to 571 years for cores WP92-5, respectively. The age models for these cores were set up using *G. sacculifer* $\delta^{18}O$ stratigraphy, the Toba volcanic event, magnetostratigraphy and several ^{14}C dates. A detailed tuning of isotopic events, such as Heinrich (H) and D-O events, with those identified in core 17940 that has a much better constraint by AMS ^{14}C ages from the northern SCS [*Wang et al.*, 1999], further increases the accuracy of the age models for the three cores studied.

[31] Although the sediment record of the last 2000 years (in NS93-5) and 6000 years (in WP92-5) is largely missing, the early part of MIS 1 registers average $\delta^{18}O$ of about −2.8‰ at NS93-5 (minimum −3.3‰) and about −2.3‰ at WP92-5 (minimum −2.75‰). A similar average $\delta^{18}O$ value of about −1.5‰ is recorded in MIS 2 of both cores, about 0.2‰ more negative than that from core 17940 in the northern SCS. The average $\delta^{18}O$ values for MIS 3 from NS93-5 and WP92-5 mimic their MIS 1 values. These isotopic variations from MIS 3 to MIS 1 reflect the impact of climate and particularly the East Asian monsoons. It may be inferred from this work that a portion of these $\delta^{18}O$ changes in NS93-5 from SCS can be ascribed to SSS changes due to a prevailing summer monsoon in warmer or interglacial periods, and a prevailing winter monsoon during cooler or glacial periods. For the core WP92-5 record, from the central WPWP, ice volume changes combined with different climate circulation modes in the open western Pacific as a result of glacial-interglacial variations are more obvious and therefore the record contains more global components.

[32] A variable WPWP from MIS 3 to MIS 1 is also indicated by SST estimates using transfer function FP-12E. Not surprisingly, the winter SST in the central WPWP remained high throughout the three periods compared to the SCS record. In the early to mid-Holocene, winter SST in the open western Pacific ranged from 27.5°C to near 29°C with small fluctuations, but in the southern SCS it barely reached 26.5°C, indicating 2 to >3°C differences between these two areas. While their average summer SST remained relatively stable, the winter SST dropped significantly during the LGM, resulting in seasonal temperature differences of 3–4.5°C at both localities. Similar to today, the lower SST in the southern SCS was affected by the east Asian winter monsoon, which caused the lower temperatures not only in winter but also in parts of the summer. The similar magnitude of the SST decrease in both the southern SCS and central WPWP during the LGM may imply a strong glacial forcing that influenced to a similar degree the SST change from similar latitude areas.

[33] At the MIS 2/3 transition, winter and summer SST increased abruptly in the southern SCS but winter SST decreased in the central WPWP, resulting in a higher annual SST in the SCS than in the open western Pacific (Figure 8). The annual SST decrease to below 28°C in the central WPWP between 29 and 25 ka and again between 22.5 and 16.5 ka indicates an unstable warm pool that had contracted considerably, and probably shifted westward next to the

southern SCS for several thousand years during the last glacial.

[34] **Acknowledgments.** We thank Brad Opdyke and anonymous referees for reviewing the manuscript and helpful comments, and especially Larry C. Peterson for his editorial suggestions that improved the paper. This work was supported by the Knowledge Innovation Project of the Chinese Academy of Sciences (KZCX3-SW-220), the National Natural Science Foundation of China (40476024), the National Key Project for Basic Research of China (2000078500), and the Ministry of Science and Technology of China (2001DIA50041).

References

Anderson, D. M., W. L. Prell, and N. J. Barratt (1989), Estimates of sea surface temperature in the coral sea at the Last Glacial Maximum, *Paleoceanography*, *4*(6), 615–627.

Andree, M., et al. (1986), AMS radiocarbon dates on foraminifera from deep sea sediments, *Radiocarbon*, *28*(2A), 424–428.

Broecker, W. S., M. Andree, G. Bonani, W. Wolfli, M. Klas, A. Mix, and H. Oeschger (1988a), Comparison between radiocarbon ages obtained on coexisting planktonic foraminifers, *Paleoceanography*, *3*(6), 647–657.

Broecker, W. S., M. Andree, M. Klas, G. Bonani, W. Wolfli, and H. Oeschger (1988b), New evidence from the South China Sea for an abrupt termination of the last glacial period, *Nature*, *333*, 156–159.

Chen, M., and S. Chen (1989), On carbonate dissolution and the distribution model of deep sea sediment types in South China Sea (in Chinese with English abstract), *Tropic Oceanol.*, *8*(3), 20–26.

Chen, M., X. Tu, F. Zheng, W. Yan, X. Tang, J. Lu, B. Wang, and M. Lu (2000), Relations between sedimentary sequence and paleoclimatic changes during last 200 ka in the southern South China Sea, *Chin. Sci. Bull.*, *45*(14), 1334–1340.

Chen, M., R. Wang, J. Han, and J. Lu (2003), Development of east Asian summer monsoon environment revealed by radiolarians in the late Miocene: Evidence from site 1143 of ODP Leg 184, *Mar. Geol.*, *201*, 169–177.

Clement, B. M. (2004), Dependence of the duration of geomagnetic polarity reversals on site latitude, *Nature*, *428*, 637–640.

CLIMAP Project Members (1981), *Seasonal Reconstruction of the Earth's Surface at the Last Glacial Maximum*, *Map and Chart Ser.*, vol. 36, Geol. Soc. of Am., Boston, Mass.

Duplessy, J. C., E. Bard, M. Arnold, N. J. Shackleton, J. Duprat, and L. Labeyrie (1991), How fast did the ocean-atmosphere system run during the last deglaciation?, *Earth Planet. Sci. Lett.*, *103*, 27–40.

Grootes, P. M., and M. Stuiver (1997), $^{18}O/^{16}O$ variability in Greenland snow and ice with 10^{-3} to 10^{-5} yr time resolution, *J. Geophys. Res.*, *102*(C12), 26,455–26,470.

Heath, G. R. (1970), Calcite: Degree of saturation, rate of dissolution and the compensation depth in the deep oceans, *Geol. Soc. Am. Bull.*, *81*(10), 3157–3160.

Huang, C.-Y., P.-M. Liew, M. Zhao, T.-C. Chang, C.-M. Kuo, M.-T. Chen, C.-H. Wang, and L.-F. Zheng (1997), Deep sea and lake records of the southeast Asian paleomonsoons for the last 35 thousand years, *Earth Planet. Sci. Lett.*, *146*, 59–72.

Huang, C. Y., C. C. Wang, and M. X. Zhao (1999), High-resolution carbonate stratigraphy of IMAGES core MD972151 from South China Sea, *Terr. Atmos. Ocean Sci.*, *10*, 225–238.

Jacobs, J. A. (1994), *Reversals of the Earth's Magnetic Field*, 2nd ed., pp. 97–103, Cambridge Univ. Press, New York.

Jian, Z., Y. Saito, P. Wang, B. Li, and R. Chen (1998a), Shifts of the Kuroshio axis over the last 20000 years, *Chin. Sci. Bull.*, *43*, 1053–1056.

Jian, Z., M. Chen, H. Lin, and P. Wang (1998b), Stepwise paleoceanographic changes during the last deglaciation in the southern South China Sea: Record of stable isotope and microfossils, *Sci. Chin. D*, *41*, 187–194.

Jian, Z., L. Wang, M. Kienast, M. Sarnthein, K. Wolfgang, H. Lin, and P. Wang (1999), Benthic foraminiferal paleoceanography of the South China Sea over the last 40,000 years, *Mar. Geol.*, *156*, 159–186.

Jian, Z., et al. (2000), Foraminiferal responses to major Pleistocene paleoceanographic changes in the southern South China Sea, *Paleoceanography*, *15*, 229–243.

Jian, Z., B. Huang, W. Kuhnt, and H. Lin (2001), Late Quaternary upwelling intensity and east Asian monsoon forcing in the South China Sea, *Quat. Res.*, *55*, 363–370.

Kienast, M., S. Steinke, K. Stattegger, and S. E. Calvert (2001), Synchronous tropical South China Sea SST change and Greenland warming during deglaciation, *Science*, *291*(5511), 2132–2134.

Lautenschlager, M., U. Mikolajewicz, E. Maier-Reimer, and C. Heinze (1992), Application of the ocean models for the interpretation of atmospheric general circulation model experiments on the climate of the Last Glacial Maximum, *Paleoceanography*, *7*(6), 769–782.

Lea, D. W., D. K. Pak, and H. J. Spero (2000), Climate impact of late Quaternary equatorial Pacific sea surface temperature variations, *Science*, *289*, 1719–1724.

Lee, M. Y., K. Y. Wei, and Y. G. Chen (1999), High-resolution oxygen isotope stratigraphy for the last 150,000 years in the southern South China Sea: Core MD972151, *Terr. Atmos. Oceanic Sci.*, *10*, 239–354.

Li, T., Z. Liu, M. A. Hall, S. Berne, Y. Saito, S. Cang, and Z. Cheng (2001), Heinrich event imprints in the Okinawa Trough: Evidence from oxygen isotope and planktonic foraminifera, *Palaeogeogr. Palaeoclimatol. Palaeoecol.*, *176*, 133–146.

Martinez, J. I., P. D. Deckker, and A. R. Chivas (1997), New estimates for salinity changes in the Western Pacific Warm Pool during the Last Glacial Maximum: Oxygen-isotope evidence, *Mar. Micropaleontol.*, *32*, 311–340.

Martinson, D. G., et al. (1987), Age dating and the orbital theory of the ice age, development of a high-resolution 0 to 300,000 years chronostratigraphy, *Quat. Res.*, *27*, 1–29.

Miao, Q., R. C. Thunell, and D. M. Anderson (1994), Glacial-Holocene carbonate dissolution and sea surface temperatures in the South China and Sulu seas, *Paleoceanography*, *9*, 269–290.

Michael, R. R., and S. Stephen (1992), Volcanic winter and accelerated glaciation following the Toba super-eruption, *Nature*, *359*(3), 50–52.

Miller, J. R., and G. L. Russell (1990), Oceanic freshwater transport during the Last Glacial Maximum, *Paleoceanography*, *5*(3), 397–407.

Miyama, T., T. Awaji, K. Akitomo, and N. Imasato (1996), A Lagrangian approach to the seasonal variation of salinity in the mixed layer of the Indonesian Seas, *J. Geophys. Res.*, *101*(C5), 12,265–12,286.

Ninkovitch, D., and W. L. Donn (1976), Explosive Cenozoic volcanism and climatic implications, *Science*, *194*, 899–906.

Nowaczyk, N. R. (1997), High-resolution magnetostratigraphy of four sediment cores from the Greenland Sea-II. Rock magnetic and relative palaeointensity data, *Geophys. J. Int.*, *131*, 325–334.

Nowaczyk, N. R., et al. (2001), Sedimentation rates in the Makarov Basin, central Arctic Ocean: A paleomagnetic and rock magnetic approach, *Paleoceanography*, *16*(4), 368–389.

Pflaumann, U., and Z. Jian (1999), Modern distribution patterns of planktonic foraminifera in the South China Sea and western Pacific: A new transfer technique to estimate regional sea-surface temperatures, *Mar. Geol.*, *156*, 41–83.

Prell, W. L. (1985), The stability of low-latitude sea-surface temperature: An evaluation of the CLIMAP reconstruction with emphasis on the positive SST anomalies, *Rep. TR025*, U.S. Dept. of Energy, Washington, D. C.

Prell, W. L., J. Imbrie, D. G. Martinson, J. J. Morley, N. G. Pisias, N. J. Shackleton, and H. F. Streeter (1986), Graphic correlation of oxygen isotope stratigraphy application to the Late Quaternary, *Paleoceanography*, *1*, 137–162.

Rampino, M. R., and S. Self (1993), Climate-volcanism feedback and the Toba eruption of ~74,000 years ago, *Quat. Res.*, *40*, 269–280.

Steinke, S., M. Kienast, U. Plaumann, M. Weinelt, and K. Stattegger (2001), A high-resolution sea-surface temperature record from the tropical South China Sea (16500–3000 yr B.P.), *Quat. Res.*, *55*, 352–362.

Steven, W. H., and P. U. Clark (2000), Tropical climate at the Last Glacial Maximum inferred from glacier mass-balance modeling, *Science*, *290*, 1747–1750.

Tang, X. Z., W. Yan, and C. Wei (1997), *Studies on Environmental Magnetics of the Sediments From Nansha Islands and Its Adjacent Sea Area, Nanhai Studia Marina Sinica* (in Chinese), vol. 12, pp. 25–38, S. Chin. Sea Inst. of Oceanol., Chin. Acad. of Sci., Beijing.

Tang, X., Z. Chen, W. Yan, and M. Chen (2003), Younger Dryas and Heinrich events recorded by magnetic susceptibility of sediments from the central temperature area of Western Pacific Warm Pool, *Chin. Sci. Bull.*, *48*(8), 808–813.

Tarling, D. H. (1983), Palaeomagnetism, *in British Library Cataloguing in Publication Data*, pp. 162–215, CRC Press, Boca Raton, Fla.

Thompson, P. R. (1981), Planktonic foraminifera in the west North Pacific during the past 150,000 years: Comparison of modern and

fossil assemblages, *Palaeogeogr. Palaeoclimatol. Palaeoecol.*, *35*, 241–279.

Thompson, P. R., et al. (1979), Disappearance of pink-pigmented *Globigerinoides ruber* at 120,000 yr B.P. in the Indian and Pacific Oceans, *Nature*, *280*, 554–558.

Thunell, R., and Q. Miao (1996), Sea surface temperature of the western equatorial Pacific ocean during the Younger Dryas, *Quat. Res.*, *46*, 72–77.

Thunell, R. C., Q. Miao, S. E. Calvert, and T. F. Pedersen (1992), Glacial-Holocene biogenic sedimentation patterns in the South China Sea: Productivity variations and surface water pCO_2, *Paleoceanography*, *7*(2), 143–162.

Thunell, R., D. Anderson, D. Gellar, and Q. Miao (1994), Sea-surface temperature estimates for the tropical western Pacific during the last glaciation and their implications for the Pacific Warm Pool, *Quat. Res.*, *41*, 255–264.

Ujiié, H., and Y. Ujiié (1999), Late Quaternary course changes of the Kuroshio Current in the Ryukyu Arc region, northwestern Pacific Ocean, *Mar. Micropaleontol.*, *37*, 23–40.

Ujiié, H., Y. Tanaka, and T. Ono (1991), Late Quaternary paleoceanographic record from the middle Ryukyu Trench slope, northwestern Pacific, *Mar. Micropaleontol.*, *18*, 115–128.

Visser, K., R. Thunell, and L. Stott (2003), Magnitude and timing of temperature change in the Indo-Pacific warm pool during deglaciation, *Nature*, *421*, 152–155.

Wang, L., and P. Wang (1990), Late Quaternary paleoceanography of the South China Sea: Glacial-interglacial contrasts in an enclosed basin, *Paleoceanography*, *5*(1), 77–90.

Wang, L., M. Sarnthein, H. Erlenkeuser, J. Grimalt, P. Grootes, S. Heilig, E. Ivanova, C. Pelejero, and U. Pflaumann (1999), East Asian monsoon climate during the Late Pleistocene: High-resolution sediment records from the South China Sea, *Mar. Geol.*, *156*, 245–284.

Wang, P. (1999), Response of western Pacific marginal seas to glacial cycles: Paleoceanographic and sedimentological features, *Mar. Geol.*, *156*, 5–39.

Wang, P., L. Wang, Y. Bian, and Z. Jian (1995), Late Quaternary paleoceanography of the South China Sea: Surface circulation and carbonate cycles, *Mar. Geol.*, *127*, 145–165.

Wang, P., et al. (2003), Evolution of the South China Sea and monsoon history revealed in deep-sea records, *Chin. Sci. Bull.*, *48*(23), 2549–2561.

Wei, K.-Y., T.-C. Chiu, and Y.-G. Chen (2003), Toward establishing a maritime proxy record of the East Asian summer monsoons for the late Quaternary, *Mar. Geol.*, *201*, 67–79.

Winn, K., L. Zheng, H. Erlenkeuser, and P. Stoffers (1992), Oxygen/carbon isotopes and paleoproductivity in the South China Sea during the past 110,000 years, in *Marine Geology and Geophysics of the South China Sea*, edited by X. Jin, H. R. Kudrass, and G. Pautot, pp. 154–166, China Ocean Press, Beijing.

Yan, X., C. Ho, Q. Zheng, and V. Klemas (1992), Temperature and size variabilities of the Western Pacific Warm Pool, *Science*, *258*, 1643–1645.

Yang, L., M. Chen, R. Wang, and F. Zhen (2002), Radiolarian record to paleoecological environment change events over the past 1.2 MaBP in the southern South China Sea, *Chin. Sci. Bull.*, *47*(17), 1478–1483.

Zhou, M. Q., and Z. S. Ge (1987), Discussion on polarity events of Brunhes normal polarity epoch in the Yellow Sea, *Mar. Geol. Quat. Geol.*, *7*(4), 49–56.

Zielinski, G. A., P. A. Mayewski, L. D. Meeker, S. Whitlow, and M. S. Twickler (1996), A 110,000-yr record of explosive volcanism from the GISP2 (Greenland) ice core, *Quat. Res.*, *45*(2), 109–118.

M. Chen, F. Zheng, X. Tan, and R. Xiang, South China Sea Institute of Oceanology, Chinese Academy of Sciences, Guangzhou 510301, China. (mhchen@scsio.ac.cn)

Z. Jian, Laboratory of Marine Geology, Tongji University, Shanghai 200092, China.

Q. Li, Department of Geology and Geophysics, University of Adelaide, Adelaide, SA 5005, Australia.